



For the emitter, collector, and base metals, the samples were patterned with NR71-1500PY negative PR with 80s exposure and 10s RD6 spinner development. 50 nm of AuGe, 20 nm nickel (Ni) and 50 nm Au were evaporated to form the emitter and collector contacts. Capping AuGe with nickel and a layer of gold smoothed the contact surface. Excess metal was removed using lift-off, and the wafers were again patterned. 100 nm AuZn was evaporated onto the wafer and lifted off to form the base contact. Finally the samples were placed in a 45s rapid thermal anneal (RTA).

In order to isolate the common metal, a 250 nm layer of nitride ( $\text{SiN}_x$ ) was deposited using a 20 min plasma-enhanced chemical vapor deposition (PECVD). After deposition, the samples were patterned with NR9-1000P negative PR, exposed for 8s and spinner developed for 10s with RD6. The nitride layer was etched in a PlasmaTherm RIE for 5 min at a rate of 50 nm/min to create via holes with which to contact the sample. Finally, the common metal lithography was completed in the same manner as the emitter and base metals using NR71-1500PY. 20 nm of Ti and 300 nm of Au were evaporated and excess metal was removed using lift-off.

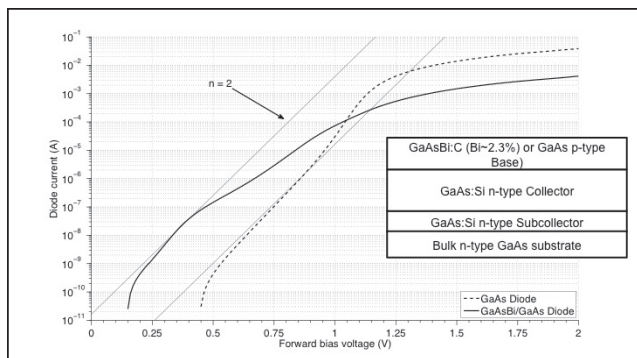


Figure 3: PN junction characteristics. PN junctions were characterized using material with a doped p-type layer of Bismuthide or GaAs on top of a doped n-type layer of GaAs and a GaAs substrate.

### Results and Conclusions:

Electrical tests of  $\text{GaAs}_{(1-x)}\text{Bi}_x$  pn junctions were conducted as shown in Figure 3. GaAs pn diodes exhibited an ideality factor of  $n = 2$  or lower, and  $\text{GaAs}_{(1-x)}\text{Bi}_x$  diodes exhibited ideal behavior at a lower turn-on voltage than the GaAs diodes corresponding to a smaller bandgap in the transistor base material as expected. The ideality factor of the  $\text{GaAs}_{(1-x)}\text{Bi}_x$  diodes rose rapidly above  $n = 2$ .

In material characterization tests,  $\text{GaAs}_{(1-x)}\text{Bi}_x$  was found to have a sheet resistance of  $2,010 \Omega/\square$ , resistivity  $\rho = 6 \times 10^{-2} \Omega\text{-cm}$  and a hole mobility of  $13 \text{ cm}^2/\text{V}\cdot\text{s}$ . Hole mobility was significantly higher in GaAs ( $93 \text{ cm}^2/\text{V}\cdot\text{s}$ ) while sheet resistance and resistivity were lower ( $450 \Omega/\square$ ,  $\rho = 1.35 \times 10^{-2} \Omega\text{-cm}$  respectively). This agrees with theory and previous material characterizations [2]. Capacitance measurements showed the material to exhibit uniform

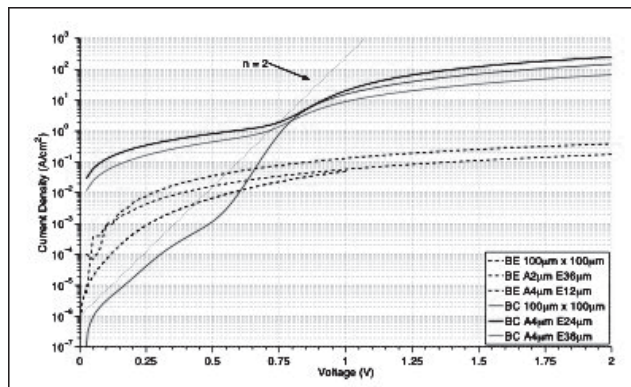


Figure 4: Base-emitter and base-collector characteristics (see Figure 2 for material structure).

doping slightly below  $10^{17} \text{ atoms/cm}^3$  as expected. The pn junction exhibited a linear relationship between applied voltage and the inverse square of capacitance.

HBT devices were fabricated with a minimum emitter mesa size of  $12 \mu\text{m} \times 100 \mu\text{m}$ . Poor contacts made devices difficult to test because the common metal deposition did not cover the large step from the subcollector to the emitter. Transistors were not achieved and diode characteristics were measured rather than true transistor curves. A thicker nitride layer or metal deposition could mitigate the issue. As shown in Figure 4 the base-collector junction exhibited ideal behavior, but the base-emitter junction showed poor rectification, possibly due to traps at the heterojunction. Future experiments are needed to improve the HBT fabrication process, particularly the contacts, and to further understand the behavior of  $\text{GaAs}_{(1-x)}\text{Bi}_x$  in the HBT base-emitter junction.

### Acknowledgements:

National Nanotechnology Infrastructure Network Research Experience for Undergraduates (NNIN REU) Program and the National Science Foundation for this opportunity, principal investigator Prof. Bart Van Zeghbroeck, mentor Ian Haygood, and Ph.D. student Zefram Marks for their knowledge and assistance. Finally thank you to CNL staff, specifically Mark Leonas.

### References:

- [1] Muller R., Kamins T., Chan M.; Device Electronics for Integrated Circuits; 3rd ed., New York: John Wiley & Sons, 2003, pp. 313-320.
- [2] Alberi, K. ;“Electronic Structure of  $\text{GaAs}_{(1-x)}\text{Bi}_x$ ”; National Renewable Energy Laboratory. Golden, Colorado. 7 June 2011. Private communication.
- [3] Williams, R.; Modern GaAs Processing Methods; 1st ed., Boston: Arctech House, 1990.